



Investigation of the association behaviors between bovine serum albumin and 2-(4-methylphenyl)-3-(*N*-acetyl)-5-(2,4-dichlorophenoxy)methyl)-1,3,4-oxodiazoline

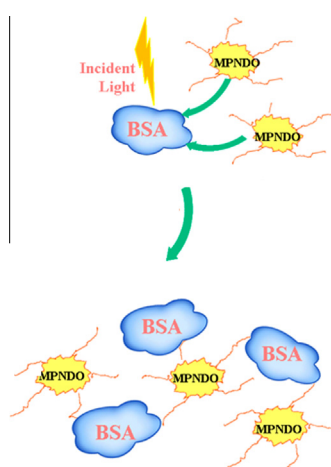
Zhenzhong Huang^{*}, Ruiling Wang, Erwei Han, Lifan Xu, Yonghai Song

College of Chemistry and Chemical Engineering, Jiangxi Normal University, Nanchang 330022, China

HIGHLIGHTS

- We have synthesized a new compound MPNDO.
- Formation of BSA–MPNDO bioconjugates were monitored by atomic force microscope.
- The work was studied by several measurements.

GRAPHICAL ABSTRACT



ARTICLE INFO

Article history:

Received 25 December 2012
Received in revised form 16 March 2013
Accepted 2 April 2013
Available online 10 April 2013

Keywords:

2-(4-Methylphenyl)-3-(*N*-acetyl)-5-(2,4-dichlorophenoxy)methyl)-1,3,4-oxodiazoline
Bovine serum albumin
Atomic force microscope
Fluorescence spectroscopy
FT-IR
Circular dichroism spectroscopy

ABSTRACT

The study was designed to examine the interaction between 2-(4-methylphenyl)-3-(*N*-acetyl)-5-(2,4-dichlorophenoxy)methyl)-1,3,4-oxodiazoline (MPNDO) and bovine serum albumin (BSA) under physiological conditions by using fluorescence spectroscopy, ultraviolet absorption spectroscopy, FT-IR spectroscopy and circular dichroism spectroscopy and atomic force microscope. Spectroscopic analysis of the fluorescence emission quenching and ultraviolet absorption revealed that the quenching mechanism of bovine serum albumin by MPNDO was static quenching procedure. The binding constant and binding sites number at different temperatures were measured. The average binding distances between donor (BSA) and acceptor (MPNDO) was estimated to be 1.46 nm (301 K), based on the Förster non-radioactive energy transfer theory. An average size of 3.1 nm had a high proportion and these dots might be ascribed to BSA, some other dots with an average size of 6.6 nm might result from BSA–MPNDO bioconjugates while the average diameter of MPNDO was 1.6 nm, which was reasonable to conclude that one BSA–MPNDO bioconjugates consisted of one BSA and one MPNDO. The thermodynamic parameters, enthalpy change (ΔH), entropy change (ΔS) and free energy change (ΔG) were calculated, which indicated that the action force was mainly van der Waals forces. The data collected through synchronous fluorescence, FT-IR spectroscopy and circular dichroism spectroscopy demonstrated that the conformation of BSA was not affected obviously in the presence of MPNDO.

© 2013 Elsevier B.V. All rights reserved.

^{*} Corresponding author. Tel.: +86 13979135290.
E-mail address: fenxi5407@163.com (Z. Huang).

Introduction

1,3,4-Oxadiazolines derivatives have attracted great much attention mainly due to some of their biological properties such as insecticidal activity, antifungal activity, anti-HIV and anticonvulsive activity [1–3]. Up to now, most papers have focused on 1,3,4-Oxadiazolines derivatives, however, to our best knowledge, MPNDO, which belongs to 1,3,4-phenoxy oxazoline derivatives have not been reported. Due to the higher biological properties compared with 1,3,4-Oxadiazolines, it is significantly meaningful to obtain further product of higher activity and make a part of the early work to do some guidance for new drug synthesis. Serum albumins are the major soluble protein constituents of the circulatory system and can play a dominant role in the transport and disposition of various compounds such as metabolites, drugs, and other biologically active substances, mostly through the formation of noncovalent complexes at specific binding sites [4–6]. Thus study on the combination of serum albumin with drugs and their derivatives is of great significance not only in providing basic information about the nature of drugs and pharmacokinetics but also in explaining the relationship between the structures and functions of drugs [7]. Bovine serum albumin (BSA) is usually selected as the protein model because of the advantages of abundance, medical importance, low cost, stability, unusual ligand-binding properties, and also particularly owing to its structural homology with human serum albumin [8]. BSA is made up of 637 amino acid residues, two of which are tryptophans located at positions 134 and 212. The structure of albumin at physiological pH is predominantly α -helical (67%) with the remaining polypeptide occurring in turns and extended or flexible regions between sub-domains with no β -sheets [9]. Bovine serum albumin (BSA) is composed of three structurally homologous domains (I, II and III), each domain contains two sub-domains (A and B). Trp-134 is in the first domain and located on the surface of the molecule, while Trp-212 is in the second domains and located within a hydrophobic binding pocket [10].

The spectroscopic technique, including UV–vis absorption spectroscopy, fluorescence spectroscopy, FT-IR spectroscopy and circular dichroism spectroscopy, is of great help in studying interactions of small molecules with protein. Fluorescence assay has been widely used to investigate proteins, and because of the sensitivity of the fluorescence to the change of the biomoleculars, researchers can use fluorescence measurements to understand molecular interaction. In this paper, measurements including atomic force microscope, fluorescence quenching spectroscopy and ultraviolet absorption spectroscopy serve as aids for studying the binding mechanism and the effect of energy transfer. The conformation change of BSA was further discussed on the basis of synchronous fluorescence spectroscopy, FT-IR spectroscopy and circular dichroism spectroscopy.

Experimental

Apparatus

All fluorescence measurements were carried out on a LS55 spectrofluorimeter (PerkinElmer, USA) equipped with a TB-85 Thermo Bath (Shimadzu, Japan) and a 1.0 cm quartz cells. The emission and excitation slits were 5 nm, 10 nm, respectively, and the scan speed was 500 nm min⁻¹. The UV-vis absorption spectra were obtained from a Lambda 35 UV–vis spectrophotometer (PerkinElmer, USA) using a 1.0 cm quartz cell. AFM measurements were studied with an AJ-III AFM instrument (Aijian, Shanghai, China) in tapping mode. Standard silicon (Si) cantilevers (spring constant, 0.6–6 N m⁻¹) were used under its resonance frequency (typically, 60–150 kHz). All AFM images were acquired at room temperature

under ambient conditions. FT-IR measurement was carried out at room temperature on a Nicolet 6700 FT-IR spectrometer with a germanium attenuated total reflection (ATR) accessory (Thermo Nicolet, USA). The CD measurements were performed at 1.0 nm intervals with a MOS-450 spectrometer (Biologic, France) equipped with a 0.1 cm path-length cell at 301 K. NMR spectra were recorded on an Avance 400 (Bruker, Germany). A FE20 pH meter with a combined glass electrode (Mettler Toledo, Shanghai, China) was used for pH measurements. ESI mass spectrum was recorded using a Waters ZQ4000/2695 LC-MS spectrometer (USA). Element analysis was performed on the Vario EL III (Elementar).

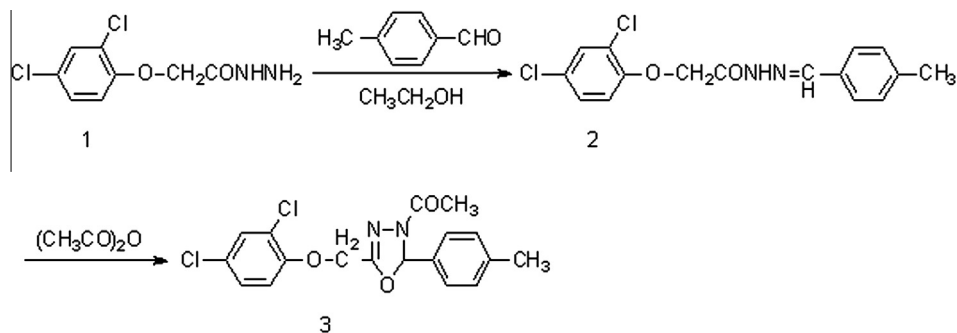
Materials

The compound MPNDO was prepared according to the reference [11] and the route for synthesis is shown in Scheme 1. Compound 2 (0.005 mol) was dissolved in acetic anhydride (20 mL) in 50 mL round bottom flask. The mixture was heated to reflux for 9 h with stirring, and then transferred into 250 mL ice water, stirred for 1 h. The precipitation was separated from the solution by filtration and recrystallized with N,N-dimethylformamide, finally, white crystals were obtained. The compound MPNDO was characterized by ¹H NMR spectrum, ¹³C NMR spectrum, IR spectrum, which were consistent with proposed formulation and the structure of MPNDO was shown in Scheme 1. The melting point (mp) was measured as 176 °C. ¹H NMR (CDCl₃, TMS): δ 2.420 (s, 3H, Ph-CH₃), 5.239 (s, 2H, COCH₂), 2.524 (s, 3H, OCH₃), 6.788–6.810 (d, 1H, J = 8.8 Hz, Ar-H), 7.145–7.167 (t, 1H, J = 8.8 Hz, Ar-H), 7.261–7.277 (d, 2H, J = 64 Hz, Ar-H), 7.387–7.393 (t, 1H, J = 24 Hz, Ar-H), 7.656–7.675 (d, 2H, J = 76 Hz, Ar-H), 8.574 (s, H, C-H). ¹³C NMR (CDCl₃): δ 21.67, 21.86, 25.97, 69.89, 114.82, 124.17, 126.82, 127.48, 128.54, 129.70, 129.85, 129.99, 130.30, 143.10, 152.62, 165.27, 168.37, 172.00. FTIR (KBr): ν /cm⁻¹ 1721 (s, C=O), 1642 (m, C=N), 1566, 1606 (m, Ar), 1278, 1067 (w, C-O-C). EIMS: *m/z* (%) = 379 [M⁺]. Elemental analyses: C₁₈H₁₆Cl₂N₂O₃, calculated C (57.01%), H (4.25%), N (7.39%), measured C (56.86%), H (4.34%), N (7.31%).

The BSA was purchased from Shanghai Rich Joint Chemical Reagents Company. The solution was prepared into a concentration of 1.0×10^{-5} mol L⁻¹ by dissolving the solid BSA in a Tris-HCl buffer. The Tris-HCl (0.05 mol L⁻¹, pH = 7.40) buffer containing 0.05 mol L⁻¹ NaCl was selected to keep the pH value constant and to maintain the ionic strength of the solution. Compound MPNDO was prepared into a concentration of 1.0×10^{-4} mol L⁻¹ in dimethyl sulphoxide (DMSO). DMSO (Alfa Aesar) is of spectrophotometric grade. All other chemicals are of analytical grade. Doubly distilled water was used throughout. All testing aqueous solution contained 1% DMSO for determination.

Procedures

A 10 μ L aqueous solution containing appropriate concentration of BSA (1.0×10^{-5} mol L⁻¹), of MPNDO (7.5×10^{-6} mol L⁻¹), of BSA-MPNDO conjugates was dropped onto a freshly cleaved mica surface, respectively. After that, the mica was rinsed with pure water and dried in air for AFM imaging. Appropriate amounts of 1.0×10^{-4} mol L⁻¹ MPNDO were added to 6 10 mL flasks, respectively, and then 1 mL of BSA solution was added and diluted to 10 mL with Tris-HCl buffer. The final concentrations of MPNDO in BSA solution were 0.0, 1.0, 2.0, 3.0, 4.0 and 5.0×10^{-6} mol L⁻¹, respectively. The resultant mixtures were then incubated at 301 K for 0.5 h. The fluorescence spectra of BSA under different concentrations of MPNDO were tested in the range of 300–500 nm upon excitation at 280 nm, each spectrum was the average of three scans. The synchronous fluorescence spectra were noted at certain scanning intervals $\Delta\lambda$ ($\Delta\lambda = 15$ nm, 60 nm). 20 μ L solution



Scheme 1. The synthesis route for MPNDO.

containing appropriate concentration of BSA ($1.0 \times 10^{-4} \text{ mol L}^{-1}$), of BSA–MPNDO conjugates was dropped on ZnSe window and dried with dry air. The FT-IR spectra of BSA in presence and absence of MPNDO taken via the ATR method with resolution of 4 cm^{-1} and 32 scans were recorded ($n = 3$ replicates) in the range of $400\text{--}4000 \text{ cm}^{-1}$. The corresponding absorbance contributions of buffer and free MPNDO solutions were recorded and digitally subtracted with the same instrumental parameters. The CD spectra of BSA ($5.0 \times 10^{-7} \text{ mol L}^{-1}$) in presence and absence of MPNDO ($1.0 \times 10^{-8} \text{ mol L}^{-1}$) were corrected for buffer absorption and recorded in the range of $190\text{--}250 \text{ nm}$, and each spectrum was the average of three scans.

Results and discussion

Mechanism of fluorescence quenching

AFM study

Formation of BSA–MPNDO bioconjugates were monitored by AFM (Fig. 1). All samples showed many small dots dispersed on mica surface uniformly and these dots might be ascribed to BSA, BSA–MPNDO bioconjugates or MPNDO. From Fig. 1A, an average size of 3.1 nm had a high proportion and these dots might be ascribed to BSA, another dots with an average size of 6.6 nm might result from BSA–MPNDO bioconjugates (Fig. 1B). Since the size of the BSA was about 3.1 nm and the size of the MPNDO was about 1.6 nm (Fig. 1C), it was reasonable to conclude that one BSA–MPNDO bioconjugates consisted of one BSA and one MPNDO. A few dots with a larger size might result from BSA–MPNDO consisted of many BSA and many MPNDO.

Fluorescence titration of BSA against MPNDO

The fluorescence spectra emission ($\lambda_{\text{ex}} = 280 \text{ nm}$, $\lambda_{\text{em}} = 345.5 \text{ nm}$) of BSA with the addition of MPNDO were obtained (shown

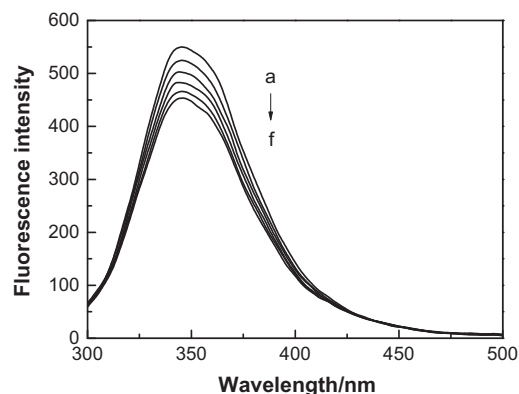


Fig. 2. Fluorescence spectra of BSA with the addition of MPNDO at 301 K. $c(\text{BSA}) = 1.0 \times 10^{-6} \text{ mol L}^{-1}$; $c(\text{MPNDO})/(10^{-6} \text{ mol/L})$, a–f: 0, 1, 2, 3, 4, 5 respectively.

in Fig. 2). The results showed that a gradual decrease in the fluorescence intensity of BSA was caused by quenching but there was no emission wavelength shift in the presence of MPNDO, the same trends were also observed at other temperatures (307 K, 313 K).

Quenching can be induced by dynamic process resulting from collisional encounters between fluorophore and quencher, or static process caused by the formation of a ground-state complex between the two compounds. Dynamic and static quenching can be distinguished by their different dependence upon the temperature of binding constants and viscosity [12]. Generally, the dynamic quenching constants are expected to increase with increasing temperature, but the reverse effect is for static quenching [12]. For dynamic quenching, the fluorescence data at different temperatures were analyzed by the well-known Stern–Volmer Equation [12]:

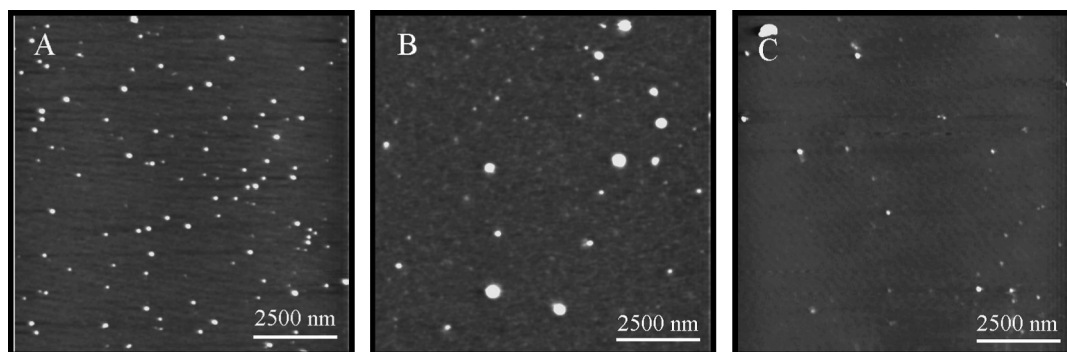


Fig. 1. AFM images of BSA (A); BSA–MPNDO (B); MPNDO (C). $c(\text{BSA}) = 1.0 \times 10^{-5} \text{ mol L}^{-1}$; $c(\text{MPNDO}) = 7.5 \times 10^{-6} \text{ mol L}^{-1}$.

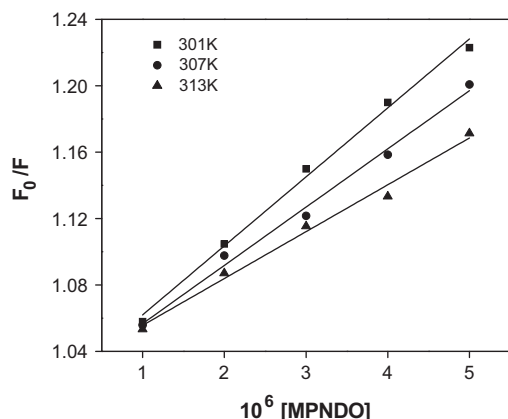


Fig. 3. The Stern–Volmer plots of the fluorescence quenching of BSA by MPNDO at different temperatures.

$$F_0/F = 1 + K_q\tau_0[Q] = 1 + K_{SV}[Q] \quad (1)$$

where F_0 and F are the fluorescence intensities in the absence and presence of drug, respectively, K_q is the biomolecular quenching rate constant, τ_0 is the average lifetime of molecule in the absence of drug and its value is 10^{-8} s [13], $[Q]$ is the drug concentration, K_{SV} is the Stern–Volmer quenching constant.

The Stern–Volmer plots are presented in Fig. 3 and the values of K_{SV} were 4.2×10^4 L mol $^{-1}$ (301 K), 3.5×10^4 L mol $^{-1}$ (307 K), 2.8×10^4 L mol $^{-1}$ (313 K), K_{SV} decreased with a rising temperature, which indicated that the fluorescence quenching mechanism may be static. The calculated quenching constants at the corresponding temperature constant K_q obtained were calculated as 4.2, 3.5, 2.8×10^{12} L mol $^{-1}$ s $^{-1}$. It was found all the values of K_q were larger than the maximum diffusion collision quenching rate constant of various quenchers with the biopolymer [14]. This result indicated that the quenching mechanism between BSA and MNPDO was mainly a static quenching process.

UV–vis absorption spectrum

UV–vis absorption measurement is also a simple but effective method in detecting static quenching and dynamic quenching [15]. As dynamic collision only affects the excited state of quenching molecules, whereas it has no influence on the absorption spectrum of quenching substance. However, ground-stated complex formation will frequently result in perturbation of the absorption spectrum of the fluorophore [13]. The absorption spectra of BSA

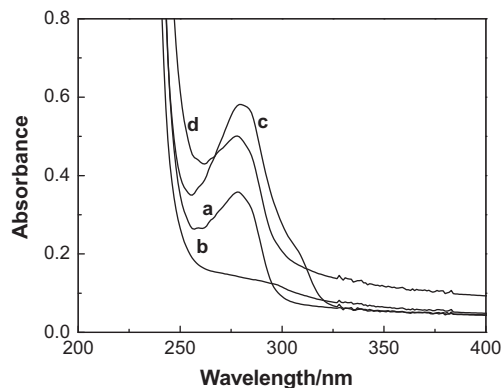


Fig. 4. UV–vis spectrum (a) the absorption spectrum of BSA only; (b) the absorption spectrum of MPNDO only; (c) the absorption spectrum BSA–MPNDO system; (d) the absorption spectrum sum of (a) and (b). $c(\text{BSA}) = 7.5 \times 10^{-6}$ mol L $^{-1}$; $c(\text{MPNDO}) = 2 \times 10^{-5}$ mol L $^{-1}$.

in the presence and absence of MPNDO are shown in Fig. 4. The absorption of BSA (curve a) is characterized by a strong band at 278 nm and MPNDO has a weak absorption band at 298 nm (curve b). Compared with curve d (sum of curve a and curve b), the addition of MPNDO led to increase in the BSA absorption with a new absorption peak at 320 nm (curve c), which may be result from the formation of a ground-state complex. The above observations further confirmed that the probable quenching mechanism between BSA and MPNDO is initiated ground-state complex formation.

Binding constant and binding sites

For static quenching, if it is assumed that there are similar and independent binding sites in the biomolecule, the binding constant and the number sites can be determined according to the method described by Chipman et al., using the following equation [16,17]:

$$\log[(F_0 - F)/F] = \log K_a + n \log[Q] \quad (2)$$

where K_a is the binding constant and n is the number sites. According to the plot of $\log(F_0 - F)/F$ versus $\log[Q]$ at different temperatures (Fig. 5), the binding constant K_a and binding sites n of MPNDO to BSA are estimated as 2.01×10^4 L mol $^{-1}$, 0.94 (301 K), 2.32×10^3 L mol $^{-1}$, 0.77 (307 K), 8.54×10^2 L mol $^{-1}$, 0.70 (313 K), respectively. The values of K_a decreased with increasing temperature, which was assumed to decrease the stability of MPNDO–BSA complex. And the values of n decreased with increasing temperature, which might be due to changes in the protein structure with temperature [18,19].

The acting force between MPNDO and BSA

The interaction forces between a ligand and protein may include hydrophobic force, electrostatic interactions, van der Waals forces and hydrogen bonds. The thermodynamic parameters can account for main forces contributing to protein stability[20], and according to the views of Ross and Subramanian [21]: (1) $\Delta H > 0$ and $\Delta S > 0$, hydrophobic forces, (2) $\Delta H < 0$ and $\Delta S < 0$, Van der Waals interaction and hydrogen bond, (3) $\Delta H < 0$ and $\Delta S > 0$, electrostatic interactions. The enthalpy is often taken to be a constant if the temperature of system is changed a little. Van't Hoff Equations [21] are used to obtain the thermodynamic parameters.

$$\ln K_a = -\Delta H/(R T) + \Delta S/R, \quad \Delta G = \Delta H - T\Delta S = -R T \ln K \quad (3)$$

where K_a is binding constant at the different temperatures and R is the gas constant. The values of ΔH , ΔS and ΔG were calculated to be -205.2 kJ mol $^{-1}$, -602.6 J mol $^{-1}$ K $^{-1}$, -23.1 kJ mol $^{-1}$. Obviously,

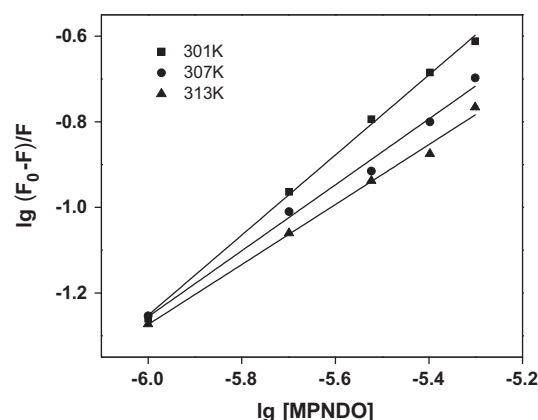


Fig. 5. The plots of $\log(F_0 - F)/F$ versus $\log c(\text{MPNDO})$ at different temperatures.

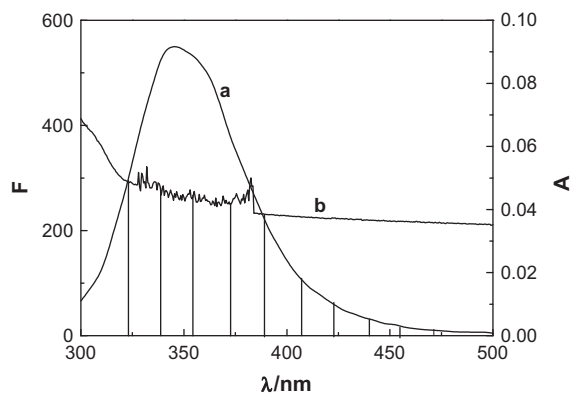


Fig. 6. Spectra overlap between the fluorescence emission of BSA (a) and the absorption spectrum of MPNDO (b). $c(\text{BSA}) = c(\text{MPNDO}) = 1.0 \times 10^{-6} \text{ mol L}^{-1}$.

both the entropy and the enthalpy were negative. So it can be concluded that the Van der Waals interaction and hydrogen bond play major roles in the acting force. However, given the structural formula of MPNDO does not contain $-\text{XH}$ ($X = \text{O}, \text{S}, \text{N}$) group, the possibility of forming hydrogen bond between BSA and MPNDO is quite low. Therefore, it can be concluded that the Van der Waals interaction was the main force during the binding of MPNDO to BSA.

Energy transfer between MPNDO and BSA

Förster's non-radioactive energy transfer theory is often used to determine the drug binding distance between the donor and acceptor under the following conditions: the donor can produce fluorescence light, the fluorescence emission spectrum of donor and the UV–vis absorption spectrum of the acceptor have enough overlap, the distance between the donor and acceptor approaches is less than 8 nm [22]. The efficiency of energy transfer (E) can be expressed according to Förster's energy-transfer theory [22]:

$$E = R_0^6 / (R_0^6 + r^6) = 1 - F/F_0 \quad (4)$$

where F and F_0 are the fluorescence intensities of BSA in the presence and absence of MPNDO, r is the distance between the acceptor and donor, and R_0 is the critical distance when the transfer efficiency is 50%. The value of R_0 was evaluated using the following equation:

$$R_0^6 = 8 \times 10^{-25} K^2 \Phi N^{-4} J \quad (5)$$

where K^2 is the spatial orientation factor of the dipole, N is the refractive index of the medium, Φ is the fluorescence quantum yield

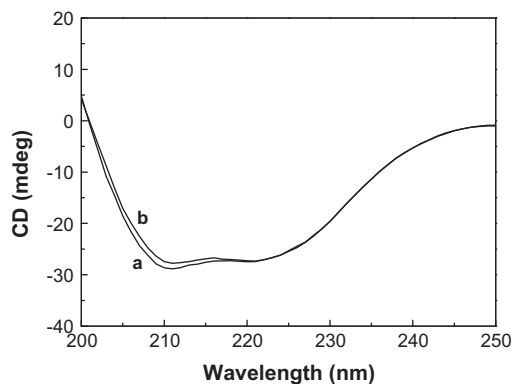


Fig. 8. CD spectra of BSA in the absence and presence of MPNDO $c(\text{BSA}) = 5.0 \times 10^{-7} \text{ mol L}^{-1}$; $c(\text{MPNDO}) = 1.0 \times 10^{-8} \text{ mol L}^{-1}$.

of the donor, and J expresses the degree of spectral overlap between the donor emission and the acceptor absorption. J could be calculated by the equation:

$$J = \sum (F_D(\lambda) \epsilon_A(\lambda) \lambda^4 \Delta\lambda) / \sum (F_D(\lambda) \Delta\lambda) \quad (6)$$

where $F(\lambda)$ is the fluorescence intensity of the fluorescent donor of wavelength λ and $\epsilon(\lambda)$ is the molar absorption coefficient of the acceptor at wavelength λ . In the present case, $K^2 = 2/3$, $N = 1.336$, and $\Phi = 0.15$ for BSA [23]. The overlap of the fluorescence emission spectrum of BSA and the absorption spectrum of MPNDO are shown in Fig. 6, together with above equations, we could obtained these parameters: $J = 9.10 \times 10^{-14} \text{ cm}^3 \text{ L mol}^{-1}$, and the binding distance r between MPNDO and the BSA is found to be 1.46 nm, indicating that the energy transfer from BSA to MPNDO occurred.

Conformational investigation

Synchronous fluorescence spectral change of BSA

The synchronous fluorescence spectrum can give only the tyrosine residues and the tryptophan residues of BSA when the wavelength interval ($\Delta\lambda$) is 15 nm and 60 nm, respectively [24]. The shift in position of maximum emission wavelength correspond to changes of the polarity around the chromospheres molecule, red shift of fluorescence spectrum suggests the polarity of the surrounding environment increasing, the hydrophobicity decreasing, and vice versa [18], thus the environment of amino acid residues can be studied by measuring the possible shift in maximum emission wavelength [25–26].

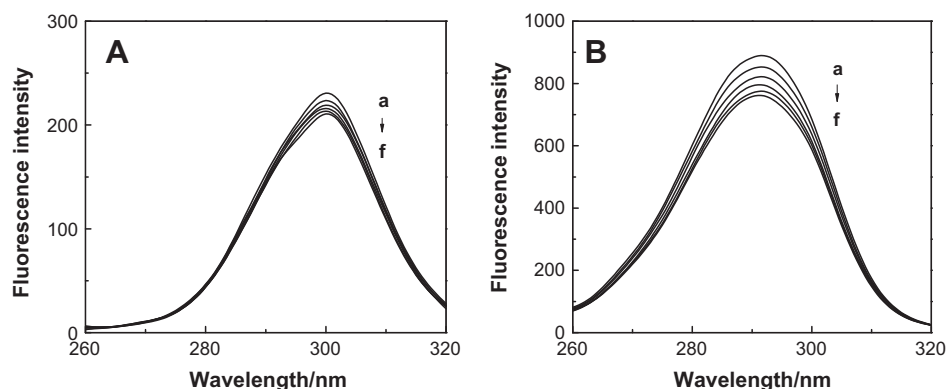


Fig. 7. Synchronous fluorescence spectra of BSA in the presence of MPNDO. ((A) $\Delta\lambda = 15 \text{ nm}$ and (B) $\Delta\lambda = 60 \text{ nm}$). $c(\text{BSA}) = 1.0 \times 10^{-6} \text{ mol L}^{-1}$; $c(\text{MPNDO})/(10^{-6} \text{ mol/L})$, a–f: 0, 1, 2, 3, 4, 5, respectively.

The synchronous fluorescence spectra were measured at $\Delta\lambda = 15$ nm and $\Delta\lambda = 60$ nm and presented in Fig. 7. As it can be seen that the emission peak intensity of BSA gradually declines upon addition of the MPNDO, while no significant shift change on maximum emission wavelength was observed. These experimental results indicated that the protein conformation was not affected obviously during the binding process.

Fourier Transform Infrared (FT-IR) study

Infrared spectrum of a protein exhibit a number of amide bands, which represent different vibrations of the peptide moiety. Among all amide modes of the peptide group, the single most widely used one in studies of protein secondary structures is the amide I. The amides I and II peak occur in the region of 1600 – 1700 cm^{-1} and 1500 – 1600 cm^{-1} , respectively. Amide I band is more sensitive to the changes in protein secondary structure compared to amide II. Hence, the amide I band is more useful for the study of protein secondary structure [27–30]. FT-IR spectra of BSA (1.0×10^{-4} mol L^{-1}) were recorded with and without the addition of MPNDO. No changes were observed in the spectra of the amide I and N–H residual amide II bands, which were present at 1656 and 1557 cm^{-1} , respectively (data not shown). This further confirmed that no changes to the secondary structure of BSA had occurred because of the interaction with the MPNDO.

Circular Dichroism (CD) study

Additional evidence regarding no conformational changes of BSA in the presence of MPNDO came from the Circular Dichroism (CD) spectroscopy, one of the valuable methods for better understanding protein secondary structure. To obtain an insight into the conformational behavior of BSA in presence and absence of MPNDO, CD spectroscopic measurements were performed. The CD spectrum of BSA exhibited two negative bands at 210 and 222 nm (curve a in Fig. 8), which is characteristic of α -helical in the advanced structure of the protein [31]. The band at 208 nm corresponds to π – π^* transition of the α -helical, whereas the band at 222 nm corresponds to π – π^* transition for both the α -helical and random coil [32]. It is clearly evident from Fig. 8 that CD spectrum of BSA (curve a) remains essentially similar to that of the BSA-MPNDO conjugates (curve b) confirming no perturbation in the secondary structure of the protein after the conjugation with MPNDO.

Conclusions

In this paper, a new compound, 2-(4-methylphenyl)-3-(*N*-acetyl)-5-(2,4-dichlorophenoxyethyl)-1,3,4-oxadiazoline was synthesized and the interaction between MPNDO and BSA has been studied. The intrinsic fluorescence of BSA has been quenched by MPNDO through static quenching mechanism. The average diameter of BSA-MPNDO changed to be 6.6 nm from 3.1 nm (BSA), 1.6 nm (MPNDO), the binding constant, binding sites number and average binding distances between BSA and MPNDO at different temperatures were obtained. The thermodynamic parameters indicated that the action force was mainly van der Waals forces. The microenvironment and conformation of BSA were demonstrated not to be changed obviously in the presence of MPNDO by synchronous fluorescence spectra, FT-IR spectra, and circular dichroism spectroscopy.

Acknowledgements

We thank the National Natural Science Foundation of China (No. 20905032) and the Research Program of Jiangxi Province Department of Education (GJJ12201) for the financial support.

References

- [1] S. Rohas, N. Gulerman, H. Erdeniz, Synthesis and antimicrobial activity of some new hydrazones of 4-fluorobenzoic acid hydrazide and 3-acetyl-2,5-disubstituted-1,3,4-oxadiazolines, *Farmaco* 57 (2002) 171–174.
- [2] J.H. Michael, P.Y. Chanyaputhipong, Preparation and Spectroscopic of 3-Xcyl-1,3,4-oxadiazolines, *Heterocyclic Chem.* 32 (1995) 1647–1649.
- [3] F.M. Liu, J.X. Ye, Synthesis of heterocyclic compounds from 2-oheny-1,2,3-triazole-4-formyl-hydrazine, *Chin. J. Chem.* 17 (1999) 62–68.
- [4] X.M. He, D.C. Carter, Atomic structure and chemistry of human serum albumin, *Nature* 358 (1992) 209–215.
- [5] B.X. Huang, H.Y. Kim, C. Dass, Probing three-dimensional structure of bovine serum albumin by chemical cross-linking and mass spectrometry, *J. Am. Soc. Mass Spectrom.* 15 (2004) 1237–1247.
- [6] J. Zhang, X.J. Wang, Y.J. Yan, W.S. Xiang, Comparative Studies on the Interaction of Genistein, 8-Chlorogenistein, and 30,8-Dichlorogenistein with Bovine Serum Albumin, *J. Agric. Food Chem.* 59 (2011) 7506–7513.
- [7] S.Y. Shi, Y.P. Zhang, X.Q. Chen, M.J. Peng, Investigation of flavonoids [bearing different substituents on ring C and their Cu^{2+} complex binding with bovine serum albumin: structure affinity relationship aspects, *J. Agric. Food Chem.* 59 (2011) 10761–10769.
- [8] X.L. Han, P. Mei, Y. Liu, Q. Xiao, F.L. Jiang, Ran Li, Binding interaction of quinclorac with bovine serum albumin: a biophysical study, *Spectrochim. Acta A* 74 (2009) 781–787.
- [9] D.C. Carter, J.X. Ho, Structure of serum albumin: *Adv. Protein Chem.* 45 (1994) 153–203.
- [10] T. Peter, Serum albumin, *Adv. Protein Chem.* 37 (1985) 161–245.
- [11] J.F. Hu, D.J. Li, Q.H. Fu, Synthesis and characterization of 1,3,4-oxadiazolines derivatives, *J. Chongqing Univ. (Nat. Sci. Ed.)* 4 (2006) 129–132.
- [12] J.R. Lakowicz, Principles of Fluorescence Spectroscopy, third ed., Springer Press, New York, 2006.
- [13] J.R. Lakowicz, G. Weber, Quenching of fluorescence by Oxygen A probe for structural fluctuations in macromolecules, *Biochemistry* 12 (1973) 4161–4170.
- [14] M.R. Eftink, C.A. Ghiron, Fluorescence quenching studies with proteins, *Anal. Biochem.* 114 (1981) 199–212.
- [15] S.Y. Bi, D.Q. Song, Y. Tian, X. Zhou, Z.Y. Liu, H.Q. Zhang, Molecular spectroscopic study on the interaction of tetracyclines with serum albumins, *Spectrochimica Acta Part A* 61 (2005) 629–636.
- [16] M. Alain, B. Michel, D. Michel, How to illustrate ligand–protein binding in a class experiment, *Chem. Educ.* 63 (1986) 365.
- [17] D.M. Chipman, V. Grisarano, N. Sharon, The binding of oligosaccharides containing N-acetylglucosamine and N-acetylmuramic acid to lysozyme, *J. Biol. Chem.* 242 (1967) 4388–4394.
- [18] X.J. Guo, X.D. Sun, S.K. Xu, Spectroscopic investigation of the interaction between riboflavin and bovine serum albumin, *J. Mol. Struct.* 931 (2009) 55–59.
- [19] L.N. Zhang, F.Y. Wu, A.H. Liu, Study of the interaction between 2,5-di-[2-(4-hydroxy-phenyl) ethylene]-terephthalonitril and bovine serum albumin by fluorescence spectroscopy, *Spectrochim. Acta A: Mol. Biomol. Spectrosc.* (2011) 1386–1425.
- [20] S.S. Lehrer, Solute perturbation of protein fluorescence. The quenching of the tryptophyl fluorescence of model compounds and of lysozyme by iodide ion, *Biochemistry* 10 (1971) 3254–3263.
- [21] P.D. Ross, S. Subramanian, Thermodynamic of protein association reaction: forces contributing to stability, *Biochemistry* 20 (1981) 3096–3120.
- [22] T. Forster, O. Sinanglu, *Modern Quantum Chemistry*, vol. 3., Academic Press, New York, 1996.
- [23] Y.Z. Zhang, B. Zhou, Y.X. Liu, C.X. Zhou, X.L. Ding, Y. Liu, Fluorescence study on the interaction of bovine serum albumin with P-aminoazobenzene, *J. Fluoresc.* 18 (2008) 109–118.
- [24] J.N. Miller, Recent advances in molecular luminescence analysis, *Anal. Proc.* 16 (1979) 203–209.
- [25] L. Stryer, Fluorescence spectroscopy of proteins, *Science* 162 (1968) 526.
- [26] B.S. Liu, F.L. Zhao, C.L. Xue, J. Wang, Y.K. Lu, Studies on the antagonistic action between chloramphenicol and quinolones with presence of bovine serum albumin by fluorescence spectroscopy, *J. Lumin.* 130 (2010) 859–864.
- [27] S. Wi, P. Pancoka, T.A. Keiderling, Predictions of protein secondary structures using factor analysis on Fourier transform infrared spectra: effect of Fourier self-deconvolution of the amide I and amide II bands, *Biospectroscopy* 4 (1998) 93–106.
- [28] K. Rahmelow, W. Hubner, Secondary structure determination of proteins in aqueous solution by infrared spectroscopy: a comparison of multivariate data analysis methods, *Anal. Biochem.* 241 (1996) 5–13.
- [29] S.Y. Lin, Y.S. Wei, M.J. Li, S.L. Wang, Effect of ethanol or and captopril on the secondary structure of human serum albumin before and after protein binding, *Eur. J. Pharm. Biopharm.* 57 (2004) 457–464.
- [30] J.W. Brauner, C.R. Flach, R. Mendelsohn, A quantitative reconstruction of the amide I contour in the IR spectra of globular proteins: from structure to spectrum, *J. Am. Chem. Soc.* 127 (2005) 100–109.
- [31] N. Vigneshwaran, A.A. Kathe, P.V. Varadarajan, R.P. Nachane, R.H. Balasubramanya, *Langmuir* 23 (2007) 7113–7117.
- [32] V.M. Bolanos-Garcia, S. Ramos, R. Castillo, J. Xicohtencatl Cortes, J.J. Mas-Oliva, *Phys. Chem. B* 105 (2001) 5757–5765.